Chapter 10
Measurement of Vibration Resulting from Non-contact Ultrasound Radiation Force

Thomas M. Huber, Spencer M. Batalden, and William J. Doebler

Abstract In modal testing, the most common excitation method is a transducer in mechanical contact with the object under test. While this method is effective, there are delicate structures where it is desirable to excite vibrations without physical contact. The ultrasound radiation force provides a noncontact excitation method resulting from the nonlinear interaction of sound waves scattering from an object. The incident ultrasound consists of sine waves with frequencies of f_1 and f_2; the resulting radiation force has a component at the difference frequency $f_1 - f_2$. By combining the difference frequency radiation force with a scanning vibrometer, previous studies have demonstrated completely non-contact measurements of resonance frequencies and operating deflection shapes of structures ranging from microcantilevers to classical guitars. In the current study, a 19.6 by 8.1 by 0.37 mm clamped-free brass cantilever, with a resonance frequency of 610 Hz, was excited using the radiation force from a focused ultrasound transducer. By mounting the transducer on a computer-controlled translation stage, it enabled measurements of the edge-spread function for the transducer; measuring this distribution is an important first step towards quantifying the applied radiation force.

Keywords Ultrasound • Radiation force • Edge-spread function • Vibrometer • Cantilever

10.1 Introduction

In modal testing of small objects, one challenge can be to excite the vibrational modes without distortions due to mass loading. Using a laser Doppler vibrometer, it is relatively straightforward to measure the vibration in a non-contact manner; however, it is not always possible to excite these vibrations without contact. The ultrasound radiation force is a non-contact method of excitation resulting from ensonifying a structure with a pair of ultrasound frequencies with the frequency difference adjusted to the resonance frequency of the structure. Previous studies have demonstrated that this technique can be used in modal testing in air for structures as small as microcantilevers [1] to as large as the face of a classical guitar [2]. These previous studies demonstrated the feasibility of determining resonance frequencies of structures, and also operating deflection shapes using a laser Doppler vibrometer. They, did not, however, quantify the magnitude or distribution of the applied radiation force.

The current study focused on using the ultrasound radiation force applied to a cantilever to directly measure the edge-spread function for an ultrasound transducer. Similar to its definition in optics, the edge-spread function is a measure of the integrated force distribution for a sharp-edged section of the circular ultrasound focus point. In the current study, this was determined by translating the ultrasound focus point across the edge of a cantilever, and monitoring the resulting radiation force using a single-point vibrometer.

10.2 Theory

Previous papers have described in detail the mechanism for ultrasound stimulated audio-range excitation, both in air [3] and in water [4–6]. If an object is ensonified with a pair of ultrasound frequencies, f_1 and f_2, interference between the two frequencies produces a radiation force that results in a vibration of the object at the difference frequency $\Delta f = f_2 - f_1$. Both frequency components were emitted from a single transducer using a double-sideband suppressed-carrier amplitude

T.M. Huber (✉) • S.M. Batalden • W.J. Doebler
Department of Physics, Gustavus Adolphus College, 800 College Avenue, Saint Peter, MN 56082, USA
e-mail: huber@gac.edu

M. Mains (ed.), *Topics in Modal Analysis, Volume 10*, Conference Proceedings of the Society for Experimental Mechanics Series, DOI 10.1007/978-3-319-15251-6_10

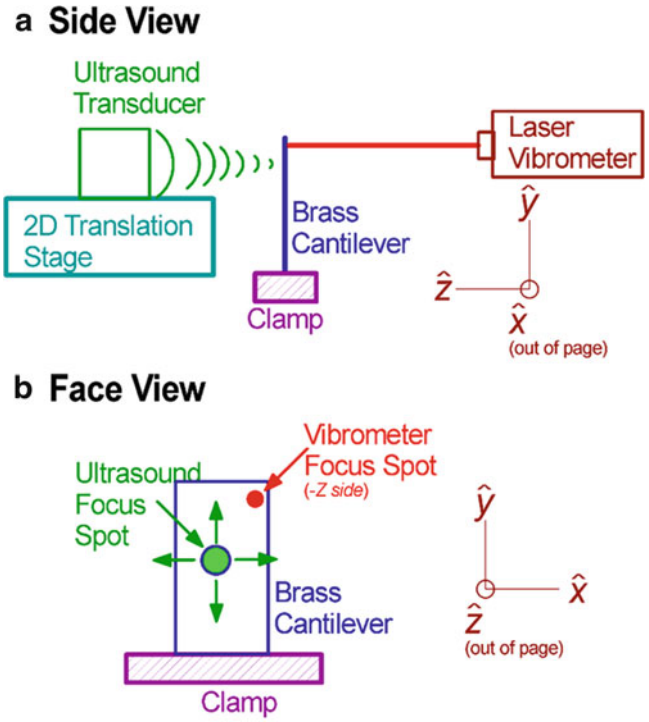

Fig. 10.1 Schematic diagram of apparatus used for measuring edge-spread functions for ultrasound radiation force excitation

modulated (AM) waveform [7, 8]. As shown in Fig. 10.1, an object was excited by a transducer emitting two different ultrasound frequencies $f_1 = f_c - \Delta f/2$ and $f_2 = f_c + \Delta f/2$ where f_1 and f_2 are ultrasound frequencies which are symmetrical about a central frequency f_c.

The radiation force [9, 10] is caused by changes in the energy density of an acoustic field. In the following derivation, it is assumed that the total ultrasound pressure field $P(\boldsymbol{r})$ at a point $\boldsymbol{r}$ will be the same at both frequencies f_1 and f_2 that are emitted by the transducer. However, as the waves of different frequencies traverse the distance between the transducer and the arrival point $\boldsymbol{r}$, they will arrive with different phases $\varphi_1(\boldsymbol{r})$ and $\varphi_2(\boldsymbol{r})$, thus the total pressure field due to the two frequency components may be written as

$$p(\boldsymbol{r},t) = P(\boldsymbol{r}) \cos[2\pi f_1 t + \varphi_1(\boldsymbol{r})] + P(\boldsymbol{r}) \cos[2\pi f_2 t + \varphi_2(\boldsymbol{r})]. \tag{10.1}$$

This causes an instantaneous energy density given by $e(r,t) = p(r,t)^2/\rho c^2$; this energy density will have a time-independent component, a component at the difference frequency Δf, and high-frequency components at multiples of f_1 and f_2. The radiation force of interest for the current technique is the energy density component at the difference frequency, which can be written as

$$e_{\Delta f}(\boldsymbol{r},t) = P(\boldsymbol{r})^2 \cos\left[\left(2\pi\Delta f\right)t + \Delta\varphi(\boldsymbol{r})\right]/\rho c^2. \tag{10.2}$$

Assuming that $P(\boldsymbol{r})$ is a plane wave, this will impart a force in the beam direction on an object of area dS with drag coefficient $d_r(\boldsymbol{r})$ given by [9, 10]

$$F_{\Delta f}(\boldsymbol{r},t)\,dS = e_{\Delta f}(\boldsymbol{r},t)\,d_r(\boldsymbol{r})\,dS = P(\boldsymbol{r})^2 \cos\left[\left(2\pi\Delta f\right)t + \Delta\varphi(\boldsymbol{r})\right]/\rho c^2\; d_r(\boldsymbol{r})\,dS. \tag{10.3}$$

The total radiation force $F_{Tot,\Delta f}(r,t)$ as a function of time is the integral of Eq. 10.3 over the ensonified surface of the object; this radiation force can induce a vibration of the object at a frequency Δf. Object vibration due to this radiation force is a function of the size, shape and mechanical impedance of the object. Previous studies have shown that this radiation force can be used for modal analysis of a variety of systems [11–13] including hard-drive suspensions [14–16]. To eliminate standing waves between the transducer and surface, the frequencies f_1 and f_2 were rapidly varied using a random carrier packet algorithm that maintained the difference frequency Δf [17].

The ultrasound radiation force distribution $F_{\Delta f}(r,t)$ from a circular focused transducer will have a radial distribution function with a central circular maximum, surrounded by successive rings of minima and maxima. If this circular beam focus, centered at (x_s,y_s), overlaps a section at the edge of a cantilever with known drag function $d_r(\boldsymbol{r})$ that is centered at $x=0$ and parallel to the y axis, the total radiation force would then be a fraction of the circular beam distribution given by

$$F_{\mathrm{Tot},\Delta \mathrm{f}}\left(x_s, y_s, \mathrm{t}\right) = \iint\limits_{x>0,y} F_{\Delta \mathrm{f}}\left(x - x_s, y - y_s, \mathrm{t}\right) d_r\left(x, y\right) dxdy \tag{10.4}$$

A plot of $F_{\mathrm{Tot},\Delta \mathrm{f}}(x_s, y_s, \mathrm{t})$ versus x_s as the transducer is moved across the edge at $x=0$ is called the edge-spread function. By determining this edge-spread function, it should be possible to infer the radial distribution function $F_{\Delta f}(r,t)$ which is useful in modeling the response of ultrasound on an object with a more complicated shape or unknown drag function.

For the current study, a brass cantilever was clamped at one end as shown in Fig. 10.1. According to Euler beam theory [18], the displacement of the cantilever is independent of position in the x direction. The measured deflection shape $z(y)$ along the y direction was fit to the functional form expected for a clamped-free cantilever,

$$z(y) = a\left\{\left[\sin\left(\lambda\left(y - y_0\right)\right) - \sin \mathrm{h}\left(\lambda\left(y - y_0\right)\right)\right] + b\left[\cos \mathrm{h}\left(\lambda\left(y - y_0\right)\right) - \cos\left(\lambda\left(y - y_0\right)\right)\right]\right\} \tag{10.5}$$

where y_0 is the position of the clamped edge of the cantilever, a is an amplitude parameter, the product of the parameter λ and cantilever length ℓ has the value $\lambda\ell = 1.875104$ for the fundamental mode, and b is given by

$$b = \left[\frac{\sinh\left(\lambda\ell\right) + \sin\left(\lambda\ell\right)}{\cosh\left(\lambda\ell\right) + \cos\left(\lambda\ell\right)}\right]. \tag{10.6}$$

10.3 Experimental Setup and Procedure

The apparatus used is shown schematically in Fig. 10.1. The cantilever was a strip of brass with dimensions of 19.6 by 8.1 by 0.37 mm clamped at one end in a machinist's vise. The vise had a mass of about 2 kg and was bolted to a Newport optical vibration isolation table to make a stable support.

The transducer used in this portion of the testing was a custom-made ultrasound transducer for operation in air (MicroAcoustics Instruments, Gatineau, Canada). This transducer has a focal length of 7 cm and produces a focused ultrasound spot with a beam profile roughly 2 mm in diameter. The transducer's central maximum is located near 700 kHz with a bandwidth of over 200 kHz. The transducer was attached to an orthogonal pair of Newport 423 translation stages with computer-controlled Zaber Technologies T-NA08A25 μm with 0.05 μm resolution and 25.4 mm travel. Thus, the location of the transducer focus point could be raster scanned over a range of positions extending beyond the edges of the cantilever.

The transducer's waveforms were output from a 4-channel Strategic Test UF2e-6022 60 MSamples/s Arbitrary Waveform Generator PCI express board (Stockholm, Sweden). This board generated the Double-Sideband, Suppressed Carrier (DSB-SC) waveform of Eq. 10.1 with a carrier frequency in the vicinity of 700 kHz, and a pair of sidebands separated by 610 Hz. This waveform was amplified using an ENI-240 L RF amplifier to about 250Vpp. Another DAC output channel continuously cycled a simple 610 Hz sine wave that was used as a reference signal.

To determine the vibration of the cantilever, a Polytec PSV-400 Scanning Laser Doppler Vibrometer (Waldbronn, Germany) was focused near the free end of the cantilever. The vibrometer analog output signal was routed into a Zurich Instruments HF2LI Lock-In Amplifier (Zurich, Switzerland) with the reference signal being the 610 Hz sine wave produced by the Strategic Test card.

10.4 Results

The ultrasound transducer produced a DSB-SC waveform that had a difference frequency of 610 Hz, which is the resonance frequency of the brass cantilever used. By moving the transducer using the computer-controlled translation stage system, it was possible to perform horizontal scans where the transducer was kept at a fixed position in the y direction and multiple points were taken at different x positions, as shown in Fig. 10.2. The transducer was scanned such that the ultrasound focus

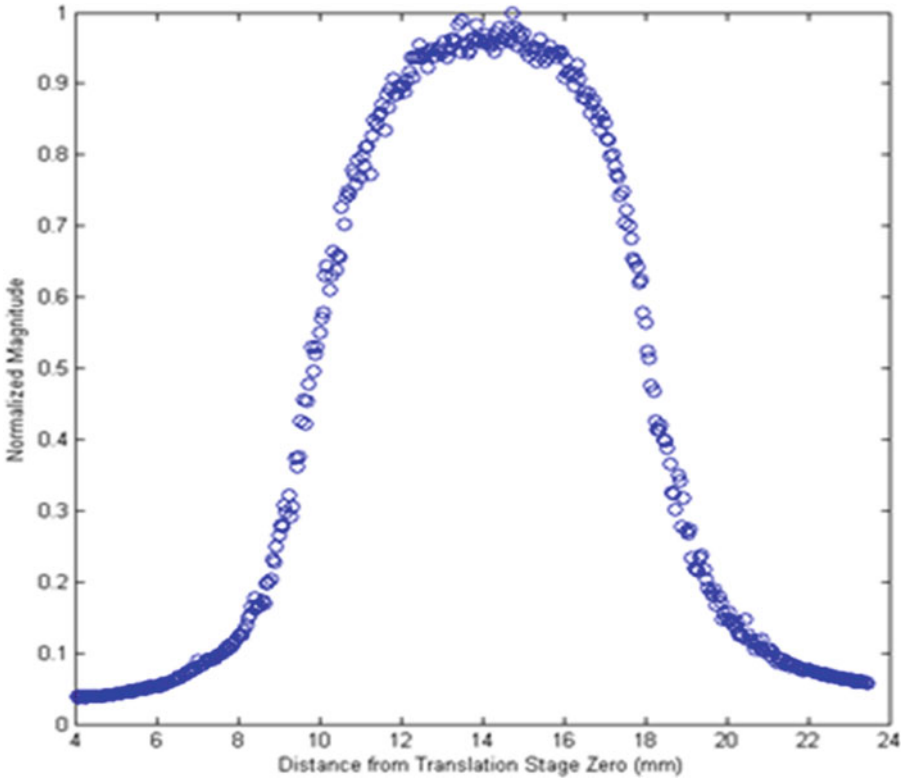

Fig. 10.2 Normalized response as ultrasound focus point is scanned across horizontal width of cantilever

point was directed beyond one edge of the cantilever, moved across the cantilever until it moved beyond the other side. The vibrometer measured the velocity amplitude corresponding to each position of the ultrasound focus point; each of these velocities were divided by the maximum velocity to produce the normalized magnitude. Since the response of a cantilever to a point force is independent of the horizontal position, the response function would have square edges that would go from 0 to 1 if the ultrasound focus point was infinitesimally small. However, because of the finite size of the ultrasound focus spot, there will be a distribution as shown in Fig. 10.2 since the cantilever's response will be reduced if a fraction of the ultrasound focus is not striking the cantilever. The normalized magnitude would be 0.5 when the center of the ultrasound focus spot was centered on the edge of the cantilever since half of the focus spot would be striking the cantilever and half would miss the cantilever off of the edge. The distance between these half-response points of 8.2 ± 0.1 mm is consistent with the 8.1 mm width of the cantilever.

Alternately, vertical scans consisted of positioning the transducer at the midpoint of the cantilever in the x direction and taking multiple measurements with varying positions in the y direction, as shown in that data points on Fig. 10.3. Even though the center of the ultrasound transducer began this scan below the clamped edge of the cantilever, the response did not go to zero because a fraction of the ultrasound focus spot was still striking the cantilever. As the transducer was moved in the positive y direction towards the free end of the cantilever, the cantilever's response would increase as expected if the driving force was concentrated at a single location. However, when the ultrasound transducers focus spot extended beyond the end of the cantilever, the applied force on the cantilever decreased, which leads to the decreasing amplitude of data points towards the right side of Fig. 10.3.

The solid line in Fig. 10.3 is a least-squares fit of a section of the data set illustrated to Eq. 10.5 which is the response expected for a point-source applied to a cantilever at a location y. The free parameters in this fit were y_0, the position of the clamped edge of the cantilever, and the amplitude parameter a. The section of the data set used for the fit was selected to insure that the majority of the ultrasound focus spot was incident on the transducer and not falling beyond the clamped or free ends of the cantilever. This fit demonstrates that, as long as the ultrasound focus point is entirely striking the cantilever, it causes a response that is essentially equivalent to a point source at that location. However, once the ultrasound focus spot extends beyond the edge of the cantilever, it is necessary to take into account the integrated response of the fraction of ultrasound incident on the surface.

The edge-spread function is defined as the integrated fraction of the radial distribution function incident on a sharp edge. Alternately, it can be modeled as a 2-d convolution between the square edge of the cantilever and the radial distribution function. Figure 10.4 shows two independent measurements of the edge-spread function determined using this

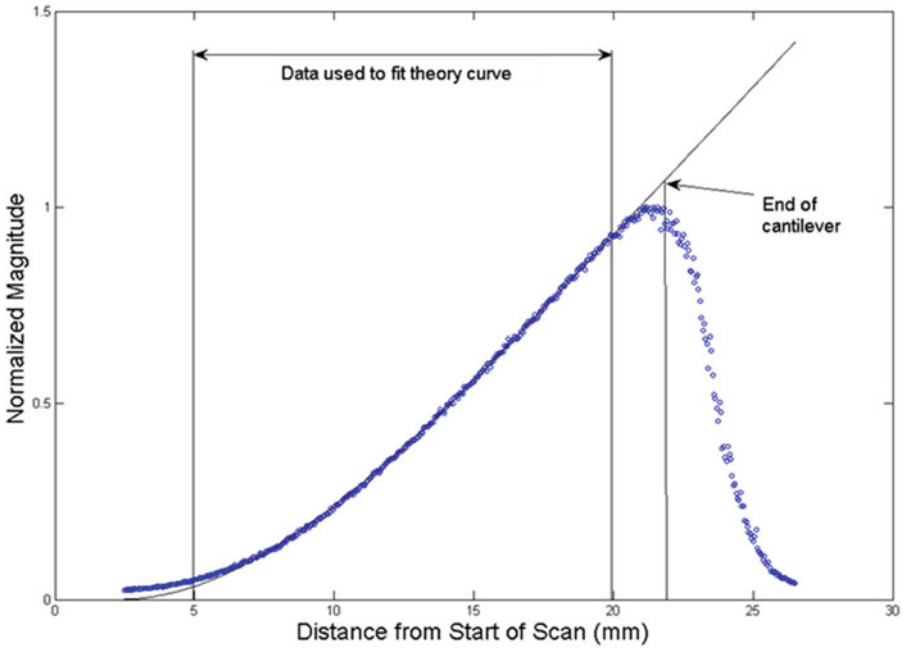

Fig. 10.3 Comparison of measurements of normalized response of cantilever as ultrasound focus point is moved along vertical axis of cantilever (*open circles*) and theoretical fit for response of cantilever to a point-source driving force (*solid line*). The reduction of response, particularly at distances above about 22 mm in this graph, is because only a fraction of the ultrasound focus point strikes the cantilever

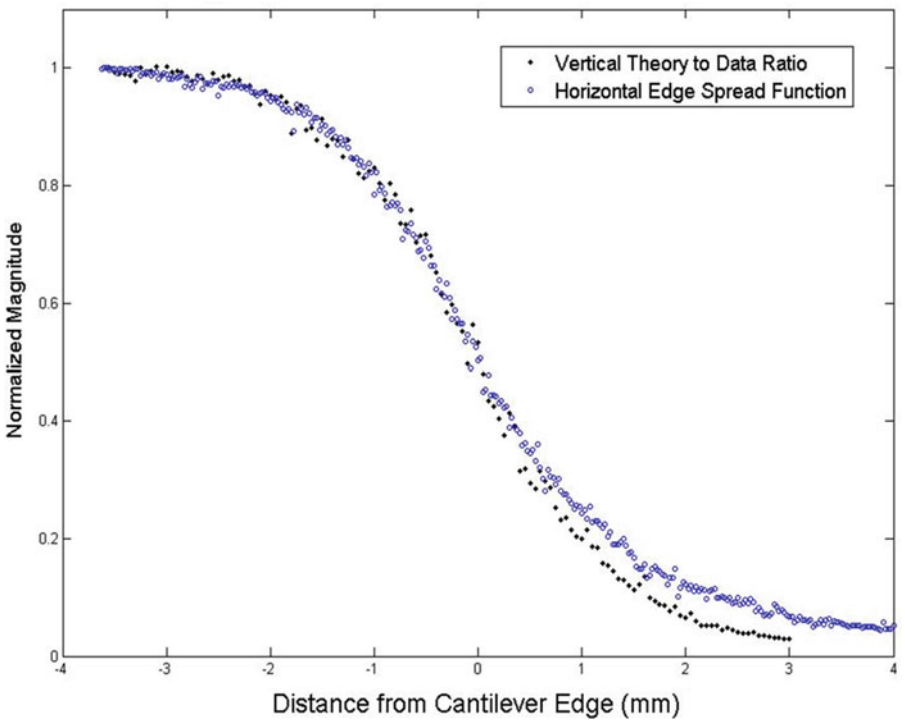

Fig. 10.4 Measurement of edge-spread function using horizontal scan (*open circles*) and vertical scan (*solid points*)

roving-transducer experiment. For the open circles, this plot shows the data set from the right-hand edge of Fig. 10.2, which is a horizontal scan across the width of the cantilever with the 50 % location shifted to correspond to $x = 0$. For negative positions less than -3 mm, essentially the entire ultrasound focus spot was striking the cantilever, thus the normalized response was essentially 1. For positive positions greater than about $+3$ mm, essentially the entire ultrasound focus spot was beyond the edge of the cantilever, leading to a very small normalized response. The shape of this curve between these limits is the measured edge-spread function for this transducer.

As an independent measurement of the edge-spread function, the vertical scan shown in Fig. 10.3 was used to determine the solid dots shown in Fig. 10.4. To create these points, the ratio between the measured response of Fig. 10.3 was divided by the theoretical prediction from a point source (solid line in Fig. 10.3). This ratio essentially measures how much the response

decreases because the actual response is an integral of a finite-sized radial distribution that might extend beyond the edge of the cantilever. The x values for this plot were the distance of the center of the ultrasound focus spot from the free end of the cantilever. Again, when the transducer was more than about 3 mm below the free end of the cantilever (−3 mm on this plot), the normalized response was about 1, and this fell to near zero once the ultrasound focus point was more than about 3 mm above the free end of the cantilever. These two independent measurements of the edge-spread function are in very good agreement. The slight variation may be due to uncertainties in determining the location where the center of the ultrasound focus is exactly at the edge of the cantilever.

10.5 Conclusions

The experiments described demonstrate that it is possible to use the ultrasound radiation force of a roving transducer moving across a fixed-free cantilever to measure the edge-spread function of an ultrasound transducer. Future studies will involve utilizing this edge-spread function to determine the radial-distribution of the ultrasound radiation force. The combination of knowing the ultrasound radiation force applied to a surface and the measured operating deflection shapes using a scanning laser Doppler vibrometer, the goal is determination of frequency response functions using a fully non-contact method for both excitation and measurement.

Acknowledgements This material is based upon work supported by the National Science Foundation under Grant Nos. 0959858, and 1300591. Any opinions, findings and conclusions or recommendations expressed in this material are those of the author(s) and do not necessarily reflect the views of the National Science Foundation (NSF). The authors would like to thank B. Bjork for preliminary measurements and assistance with some of the analysis.

References

1. Huber TM, Abell BC, Mellema DC, Spletzer M, Raman A (2010) Mode-selective noncontact excitation of microcantilevers and microcantilever arrays in air using the ultrasound radiation force. Appl Phys Lett 97:214101
2. Huber TM, Beaver NM, Helps JR (2013) Noncontact modal excitation of a classical guitar using ultrasound radiation force. Exp Tech 37(4):38
3. Huber TM, Fatemi M, Kinnick RR, Greenleaf JF (2006) Noncontact modal analysis of a pipe organ reed using airborne ultrasound stimulated vibrometry. J Acoust Soc Am 119:2476
4. Fatemi M, Greenleaf JF (1998) Ultrasound stimulated vibro-acoustic spectography. Science 28:82
5. Fatemi M, Greenleaf JF (1999) Vibro-acoustography: an imaging modality based on ultrasound-stimulated acoustic emission. Proc Natl Acad Sci 96:6603
6. Greenleaf JF, Fatemi M (1999) Acoustic force generator for detection, imaging and information transmission using the beat signal of multiple intersecting sonic beams. US Patent 5,903,516
7. Chen S, Fatemi M, Kinnick RR, Greenleaf JF (2004) Comparison of stress field forming methods for vibro-acoustography. IEEE Trans Ultrason Ferroelect Freq Control 51(3):313
8. Fatemi M, Greenleaf JF (1999) Acoustic force generation by amplitude modulating a sonic beam. US Patent 5,921,928
9. Westervelt PJ (1951) Theory of steady force caused by sound waves. J Acoust Soc Am 23:312
10. Borgnis FE (1953) Acoustical radiation pressure of plane compressional waves. Rev Mod Phys 25:653
11. Fatemi M, Greenleaf JF (2000) A novel method for modal analysis of fine structures. In: Proceedings 2000 IEEE international ultrasonics symposium short courses, p 252, Oct 2000
12. Fatemi M, Greenleaf JF (2002) Mode excitation and imaging by the radiation force of ultrasound. J Acoust Soc Am 111:2472
13. Mitri FG, Trompette P, Chapelon J-Y (2003) Detection of object resonances by vibro-acoustography and numerical vibrational mode identification. J Acoust Soc Am 114:2648
14. Huber TM, Calhoun D, Fatemi M, Kinnick RR, Greenleaf JF (2006) Noncontact modal testing of hard-drive suspensions using ultrasound radiation force. In: Proceedings of international modal analysis conference (IMAC XXIV), 2 Feb 2006, paper 363; see http://physics.gac.edu/~huber/Presentations/imac_2006_february
15. Huber TM, Calhoun D, Fatemi M, Kinnick RR, Greenleaf JF (2005) Noncontact modal testing of hard-drive suspensions using ultrasound radiation force. J Acoust Soc Am 118:1928; see http://physics.gustavus.edu/~huber/presentations/asa_2005_october/
16. Huber TM, Purdham JC, Fatemi M, Kinnick RR, Greenleaf JF (2005) Noncontact mode excitation of small structures in air using ultrasound radiation force. J Acoust Soc Am 117:2455; see http://physics.gustavus.edu/~huber/presentations/asa_2005_may/
17. Huber TM, Beaver NM, Helps JR (2011) Elimination of standing wave effects in ultrasound radiation force excitation in air using random carrier frequency packets. J Acoust Soc Am 130:1838
18. de Silva CW (2007) Vibration: fundamentals and practice, 2nd edn. CRC Press/Taylor & Francis Group, Boca Raton, pp 346–351